Interaction of the Cesium Cation with Mono-, Di-, and Tricarboxylic Acids in the Gas Phase. A Cs^+ Affinity Scale for Cesium Carboxylates Ion Pairs

Charly Mayeux,[a] Jaana Tammiku-Taul,[b] Lionel Massi,[a] Ene-Liis Lohu,[b] Peeter Burk,[b] Pierre-Charles Maria,[a] and Jean-François Gal[a]

[a] Institut de Chimie de Nice, Laboratoire de Radiochimie, Sciences Analytiques et Environnement, and Plateforme Technologique de Chimie-Spectrométrie de Masse, Faculté des Sciences, Université de Nice Sophia-Antipolis, Nice, France
[b] Institute of Chemistry, University of Tartu, Tartu, Estonia

Humic substances (HS), including humic and fulvic acids, play a significant role in the fate of metals in soils. The interaction of metal cations with HS occurs predominantly through the ionized (anionic) acidic functions. In the context of the effect of HS on transport of radioactive cesium isotopes in soils, a study of the interaction between the cesium cation and model carboxylic acids was undertaken. Structure and energetics of the adducts formed between Cs^+ and cesium carboxylate salts [Cs^+RCOO^-] were studied by the kinetic method and density functional theory (DFT). Clusters generated by electrospray ionization mass spectrometry from mixtures of a cesium salt (nitrate, iodide, trifluoroacetate) and carboxylic acids were quantitatively studied by CID. By combining the results of the kinetic method and the energetic data from DFT calculations, a scale of cesium cation affinity, CsCA, was built for 33 cesium carboxylates representing the first scale of cation affinity of molecular salts. The structural effects on the CsCA values are discussed. (J Am Soc Mass Spectrom 2009, 20, 1912–1924) © 2009 American Society for Mass Spectrometry

As products of nuclear fission, the radioisotopes of cesium ^{134}Cs and ^{137}Cs (half-lives 2.1 and 30.1 y, respectively [1]), are typical anthropogenic pollutants. Their main sources were the fallouts of the Chernobyl accident in April 1986, and the atmospheric nuclear weapons tests from 1945 to 1980. Owing to the respective half-life of these radioisotopes, ^{137}Cs is still abundant, in particular in the upper layers of uncultivated soil, like in forest litter [2–4], and is found in fungi [5] and plants [6, 7]. Cesium retention and transport in soil is primarily determined by the mineral fraction, especially clay [8], but the soil organic matter (SOM) may interfere, as shown, for example, by Dumat and Staunton and their coworkers [9, 10]. For this reason, humic substances, as components of SOM, may be considered as a significant factor in the mobility and availability of ^{137}Cs in soil. The fraction of dissolved organic matter bound to soil contributes also to cesium mobility by ion-exchange [11].

SOM is a component of the upper layers of soils and is in part constituted of humic substances, which are subdivided into fulvic and humic acids, and humin. Their structures are complex [12], but various structural models (or pseudostructures) of fulvic acids (FA) [13], and humic acids (HA) have been proposed [13, 14]. The main structural features of FA and HA are the ratio of aliphatic and aromatic carbon atoms, and the occurrence of units like phenol, quinone, amino acid, carbohydrate, and carboxylic acid, which are active in complexing metal cations [15–17]. Carboxylic acids, especially polycarboxylic acids, are known to form complexes with metal cations. For example, succinic and oxysuccinic acids are good structural models aimed at understanding metal binding by fulvic acids [18]. Additionally, several low molecular weight carboxylic acids can also be found in soil, specifically in the rhizosphere [19], and constitute a significant part of dissolved organic matter [20]. These aliphatic and aromatic mono- and polycarboxylic acids, produced in part by plant roots, could play a role in metal mobilization and uptake by plants [21]. Of note, there is some similarity between fulvic and humic acids and the soluble polymeric acids found in fog [22]. A part of carboxylic acids found in soil, especially aliphatic dicarboxylic acids, originates from atmospheric aerosol particles [23, 24].

For a better understanding of ^{137}Cs fate, its mobility and plant uptake, data on the interactions between Cs^+ and carboxylic acids, which are mainly in anionic forms in soil, would be helpful. A first step toward the description of such interactions consists in establishing

Address reprint requests to Professor J.-F. Gal, Institut de Chimie de Nice, Laboratoire de Radiochimie, Sciences Analytiques et Environnement, Faculté des Sciences, Université de Nice Sophia-Antipolis, 06108 Nice Cedex 2, France. E-mail: Jean-Francois.Gal@unice.fr

1044-0305/09/$32.00
doi:10.1016/j.jasms.2009.07.003

Published online July 14, 2009
Received April 15, 2009
Revised July 1, 2009
Accepted July 1, 2009

the intrinsic (in vacuo) properties of gas-phase Cs^+ adducts. Available data on the energetics of Cs^+ adducts in the gas phase [25] are not really pertinent to the kind of interactions we are seeking. In previous studies [26–28], we advocated that combined studies by mass spectrometry and molecular orbital calculations on the formation of cesium cation complexes with organic carboxylic acids and their anions will advance our knowledge in the field of Cs^+/SOM interactions. The experimental approach was designed to provide informations on the relative gas-phase affinities of Cs^+ toward organic moieties, by investigating the formation of Cs^+ clusters with carboxylic acids, using electrospray ionization mass spectrometry (ESI-MS). We applied the kinetic method [29, 30], scaled by theoretical (density functional theory, DFT) enthalpies (or Gibbs free energies), to establish a relative scale of cesium cation affinity (or basicity) of cesium carboxylate salts [27, 28]. The gas-phase cesium cation affinity (CsCA) and basicity (CsCB) can be defined for any species L (L stands for ligand), which may be neutral or anionic. In this work, L is a neutral, isolated ion pair $[Cs^+A^-]$ (usually simplified as [CsA] in the following text), and called hereafter molecular salt. Note that these species are written between brackets to avoid confusion with the affinity and basicity symbols. CsCA and CsCB are defined, respectively, as the enthalpy and the Gibbs free-energy of the dissociation reaction:

$$LCs^+ \rightarrow L + Cs^+ \quad (1)$$

In previous studies, CsCA and CsCB were referenced to cesium nitrate [27] or cesium iodide [28]. We obtained reasonable correlations between the results of the kinetic method and DFT calculations. In the present work, we establish CsCA and CsCB scales for 33 ligands, L = [CsA], with three different salts taken as references: cesium nitrate, cesium iodide, and cesium trifluoroacetate, using DFT (B3LYP) calculations for calibration. The three separate CsCA scales obtained with each salt are combined in one unified scale. The main structural features of the adducts are illustrated using typical geometries obtained by DFT (B3LYP) calculations. The major structural effects on the CsCA values are discussed.

Experimental

Chemicals

Methanol (LCMS grade, >99.95%) was purchased from Carl Roth (Lauterbourg, France). Ultrapure water (18.5 MQ.cm) was generated from a Millipore (Molsheim, France) MilliQ system. Cesium iodide (99.999%) and trifluoroacetate (99.4% on Cs^+ content) are from Alfa Aesar (Schiltigheim, France), and cesium nitrate (>99%) from Merck (VWR International, Fontenay-sous-Bois, France). Organic acids were obtained from Alfa Aesar, Merck, VWR, Sigma-Aldrich-Fluka (Saint-Quentin Fallavier, France), EGA-Chem (Steinheim, Germany), at the best purity available, and used without further purification.

Mass Spectrometry

The experiments were conducted in a way similar to our previous studies [26–28]. Electrospray mass spectra were recorded on a Finnigan MAT (Thermo Electron, Courtaboeuf, France) LCQ ion trap mass spectrometer, the source being operated under the following conditions: flow rate 3 μL/min; electrospray ionization voltage: 4.5 kV; capillary voltage: adjusted for each mixture of organic acid and cesium salts; capillary temperature: 200 °C; nebulizer gas: nitrogen. Cesium salts were dissolved in ultra pure water to obtain a solution at about 3 mg/mL (about 1.5×10^{-2} mol L^{-1}). Organic acids were dissolved in methanol to obtain solutions at comparable concentrations. Electrosprayed solutions were prepared from equal volumes of the aqueous cesium salt solution and a methanolic solution of the carboxylic acid. To avoid formation of methyl ester in the acid solution [31], it was necessary to use freshly prepared solutions. Acetonitrile reduces esterification [32] but is less efficient than methanol as ESI solvent in our context. The m/z range was set between 50 and 2000. Collision-induced dissociation (CID) experiments were carried out by trapping the precursor ion isolated within an m/z range of ±1.5 [33]. The buffer gas (helium) pressure was set automatically by the regulated inlet at about 1–2 $\times 10^{-3}$ Pa ($\approx 10^{-5}$ torr range, ion gauge reading). Typical operating conditions for carrying out CID (or MS/MS) experiments were: ion injection time 200 ms; activation q_z = 0.250; activation time = 30 ms; activation amplitude set at 17% of maximum voltage. From comparisons with CID results obtained with a quadrupole/time of flight instrument, these settings correspond approximately to a collision energy of 10 eV in the laboratory frame. The ion intensity ratios in the CID experiments are the mean of the values obtained in three separate experiments (consisting of about five spectra each), each spectrum resulting from the accumulation of about 40 scans (three microscans per scan). The composition of ions was inferred from CID spectra, isotopic peaks distribution, and cesium mass defect.

Computational Method

Calculations were performed using the Gaussian 03 program package [34]. For the organic acid salts, B3LYP hybrid density functional [35], which includes Becke's exchange functional and the correlation part attributable to Lee, Yang, and Parr was used with Dunning-Huzinaga valence double-ζ basis set augmented with polarization functions (D95V(d,p)) [36] on hydrogen and second period atoms (C, N, O, F), using pure Cartesian basis functions, i.e., five d-type basis functions per atom. Diffuse basis functions [37] were added to all second period atoms to allow for better

description of the distribution of electron density. For calculations involving the cesium cation, the Stuttgart-Dresden (SDD) effective core potential [38] and the accompanying basis set was used. A single set of polarization (d) functions was added to the SDD basis for Cs atom with an exponent of 0.19 as suggested by Glendening et al. [39].

As the described basis set is not available for iodine, a separate series of calculations was made on cesium halogenides (F^-, Cl^-, Br^-, and I^-), nitrate, and trifluoroacetate (for comparison) using def2-TZVP triple-ζ basis set [40] obtained from EMSL Basis Set Library [41]. For calculations involving the cesium and iodine atoms, the corresponding 46- and 28-electron effective core potentials [42, 43] were used. This basis set was designed to give similar errors all across the periodic table.

Full conformational searches, geometry optimizations, and vibrational analyses were performed for the anions, and the two different Cs^+ adducts: [CsA] and Cs^+[CsA]. All stationary points were found to be true minima (NImag = 0). Different initial positions of the metal cation were tested. The gas-phase enthalpies and Gibbs free energies of reaction (1) were calculated from the *H* and *G* values given by the Gaussian program for the two species [CsA] and Cs^+[CsA]. These thermodynamic values take into account zero-point energies, finite temperature correction (0 to 298 K) and pressure-volume work term. Unscaled frequencies from vibrational analysis were used. The general methodology was validated in a previous paper [26] by comparison between experimental and calculated cesium cation affinities and basicities for several simple species. Previously published CsCA and CsCB calculations on aliphatic dicarboxylates [27] and substituted benzoates [28] are included in this work.

Results and Discussion

Formation of Cs^+ Clusters

In our previous works [26–28], we used the kinetic method to establish relative scales of cesium cation affinity and basicity, CsCA and CsCB, for cesium carboxylate salts [CsA]. In preliminary works [26, 27], cesium nitrate was the source of Cs^+ ion and the reference of the scale. During the development of these scales, it was expected that using other cesium salts might help, either by shifting the range of accessible CsCA or CsCB values, or by enhancing cluster formation. Indeed, during a study of substituted cesium benzoates [28], we observed a more intense cluster formation with cesium iodide than with cesium nitrate. Using the cesium trifluoroacetate [CsTFA] salt as a reference salt is also a logical test in the framework of the kinetic method because of the functional similarity with the series under examination. As there is no experimental data for positioning the three reference salts in the CsCA or CsCB scales, their Cs^+ affinity and basicity were calculated at the DFT B3LYP/def2-TZVP level. The results are reported in Table 1 for these three salts and the other cesium halides.

The last three salts have relatively close CsCA values. As ligands with different structures, they may be considered as tests of the consistency of the kinetic method. Also, cesium iodide and trifluoroacetate have a lower CsCA than the nitrate and may help to extend downward the possibilities of measurements of Cs^+ affinities by the kinetic method. Due to different entropy effects for the halogenides compared with the nitrate and trifluoroacetate, the CsCA and CsCB orders of cesium iodide and trifluoroacetate are inverted, but the conclusion that cesium iodide and trifluoroacetate have weaker basicities than the nitrate remains valid. The entropy difference originates in the rotational contribution to entropy; see Supplemental Data, for Table 1, which can be found in the electronic version of this article.

The formulas of the carboxylic acids studied in the present work are shown in Scheme **1**.

They cover a variety of mono- and polyacids, with aliphatic, aromatic, and a few ethylenic compounds, representative of structures occurring in humic substances, as well as low molecular weight acids found in the rhizosphere. Typical positive ion electrospray mass spectra of solutions containing one of the reference salts and tartaric acid as an example are presented in Figure 1.

As regard to the distribution of anions in the clusters, the source spectra for this diacid are similar to those observed previously for mono- and polycarboxylic acids with [$CsNO_3$] [26, 27] and [CsI] [28]. We confirm also that [CsTFA] is a good candidate as a reference, giving intense ion signal for mixed clusters, i.e., containing both [CsTFA] and [CsRCOO]. For the determination of the relative CsCA of a cesium carboxylate, the simplest mixed cluster $[[CsX]Cs^+[CsRCOO]]^+$ is selected and submitted to CID. An example is given in Figure 2, showing the mass spectra obtained with a mixture of solutions of camphoric acid and cesium nitrate.

Among the various clusters with m/z up to about 2000 of the general formula $[Cs^+[CsNO_3]_n[CsCamphH]_m]^+$ (n = 1 to 9; m = 0 to 8), the simplest heterodimer $[Cs^+[CsNO_3][CsCamphH]]^+$ is of special interest. Its CID spectrum (Figure 2b) displays essentially two fragments: Cs^+[$CsNO_3$] and Cs^+[CsCamphH]. The intensity ratio may be utilized to approach the energetics of Cs^+ bonding to the molecular salts [27]. In addition to

Table 1. Cesium cation affinity or basicity for cesium halogenides, nitrate, and trifluoroacetate calculated by DFT (B3LYP/def2-TZVP level) (kJ/mol at 298 K)

Salt	CsCA	CsCB
$[Cs^+F^-]$	196.0	158.2
$[Cs^+Cl^-]$	163.4	125.8
$[Cs^+Br^-]$	151.6	112.9
$[Cs^+I^-]$	137.1	100.3
$[Cs^+NO_3^-]$	148.5	121.6
$[Cs^+CF_3CO_2^-]$	135.2	105.6

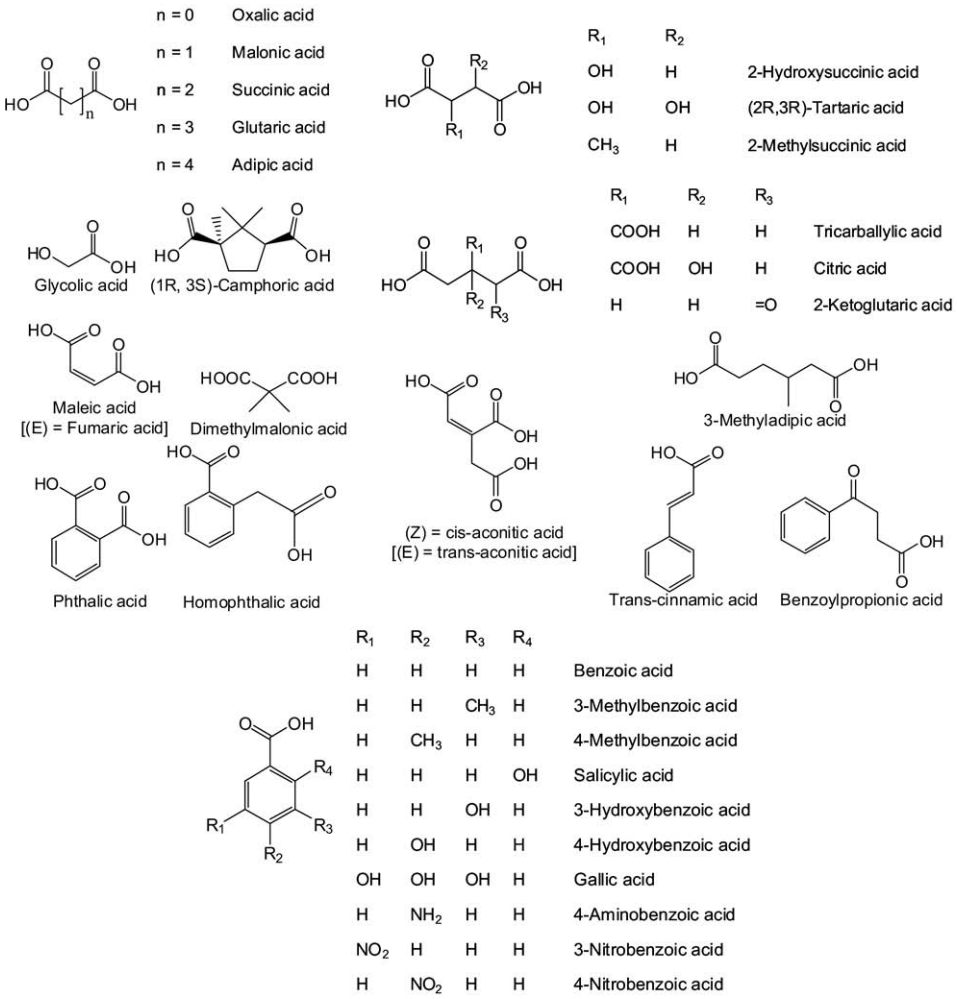

Scheme 1. Formula of the 33 carboxylic acids considered.

the expected neutral losses [CsA] and [CsX] (cesium salts), the CID spectra of the cation bound dimers exhibit also loss of $[H^+A^-]$ (here HNO_3) in the case of polyacids (or monoacids with a phenolic function) in highly variable amounts. This loss, resulting from an internal Cs^+/H^+ internal exchange within the cluster, occurs significantly in the case of tricarboxylic acids. Loss of CO_2 is also observed in the source spectra as well as the result of CID. This decarboxylation takes place primarily with malonic and dimethyl malonic acid salts. In addition to the species containing anionic form, formation of adducts between neutral carboxylic acids and Cs^+ was observed in the case of tricarboxylic acids. Adduct formation with neutral acids appears to be promoted by the number of carboxyl functions. Indeed, ESI spectra with tetracarboxylic acids (not shown) exhibit an increased abundance of such adducts.

The Kinetic Method Applied to Cs^+ Clusters

According to the kinetic method [29], the ratio of the intensities of the ions $Cs^+[CsNO_3]$ and $Cs^+[CsCamphH]$ in Figure 2b are related to the relative Cs^+ affinities (or basicities) of $[CsNO_3]$ and [CsCamphH]. It is assumed that a central Cs^+ cation is bound to the two molecular salts and that the two [CsA]–Cs^+ bonds dissociate much more rapidly than other (stronger) bonds in the cluster. As suggested by a referee, another isomeric (tautomeric) form of heterodimer, a proton-bound dimer, may be postulated in the case of polyacids. For example, camphoric acid may produce a dimer formally written as $[H^+[Cs^+NO_3^-][Cs^+Camph^{2-}Cs^+]]^+$. CID of such species might produce $H^+[CsNO_3]$ (not observed) and H^+[CsCamphCs], an isobar (tautomer) of Cs^+[CsCamphH], inducing a bias in the kinetic method. Owing to the respective proton and cesium cation affinities of anions, we do not believe that this isomer exists for the present systems, although they may be produced as higher energy intermediate(s) for the proton transfer necessary for the mentioned $[H^+A^-]$ loss.

In the CID spectrum of the Cs^+ cation-bound dimer, the two fragments are formed with unimolecular rates constants k_0 and k corresponding respectively to the formation of Cs^+ adducts with the reference salt ($[CsNO_3]$ in the above case) and with the salt [CsA]

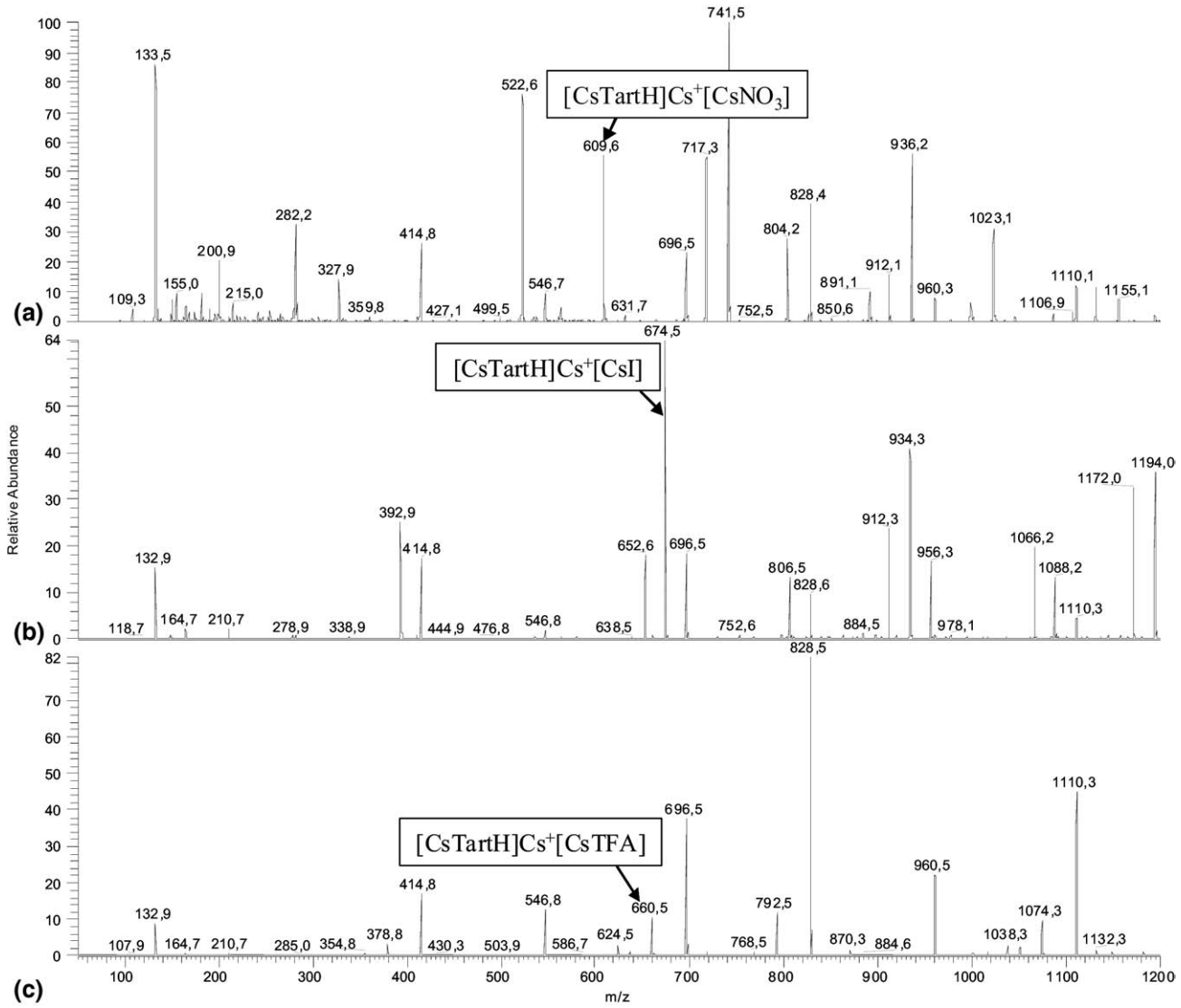

Figure 1. Electrospray mass spectra (positive mode, *m/z* range: 50–1200) of a methanol/water solution containing tartaric acid and (**a**) cesium nitrate, (**b**) cesium iodide, (**c**) cesium trifluoroacetate. The majority of ions corresponds to $[Cs^+[Cs^+X^-]_n[Cs^+TartH^-]_m[(Cs^+)_2Tart^{2-}]_p]^+$ with $TartH^-$ = hydrogen tartrate ion, $Tart^{2-}$ = tartrate ion and X^- = (**a**) nitrate, (**b**) iodide, and (**c**) trifluoroacetate ion (for simplicity, charges are removed from salt formulas on spectra).

under study (Scheme 2). Decarboxylation may compete with these fragmentations in a limited number of situations, but was not taken into account, because (1) the origin of the CO_2 loss may be the precursor (dimer) or the product ion (Cs^+ adduct), and (2) the corrections were within the experimental errors in most cases. The ratio of the two unimolecular rate constant k and k_0 is equal to the signal intensity ratio for the two product ions $Cs^+[CsA]$ and $Cs^+[CsNO_3]$, respectively I and I_0.

Cooks and coworkers [29] developed the kinetic method for obtaining quantitative data from this competitive reaction. To summarize the standard kinetic method, the branching ratio can be written as:

$$\ln(k/k_0) = \ln(I/I_0) \approx \Delta\Delta H/RT_{eff} \approx \Delta\Delta G/RT_{eff} \quad (2)$$

in which $\Delta\Delta H$ and $\Delta\Delta G$ are respectively the enthalpy and Gibbs free-energy for reaction (1) relative to the reference salt, and T_{eff} is the so-called effective temperature, which reflects the internal energy of the activated clusters ions. The implicit approximation is that $\Delta\Delta S$ is negligible. When applied to the determination of relative cesium cation affinities and basicities, one obtains:

$$\ln(k/k_0) = \ln(I/I_0) \approx \Delta CsCA/RT_{eff} \approx \Delta CsCB/RT_{eff} \quad (3)$$

The standard kinetic method can be employed when the difference in entropy of the two competitive reactions is either constant (constant reference) or negligible

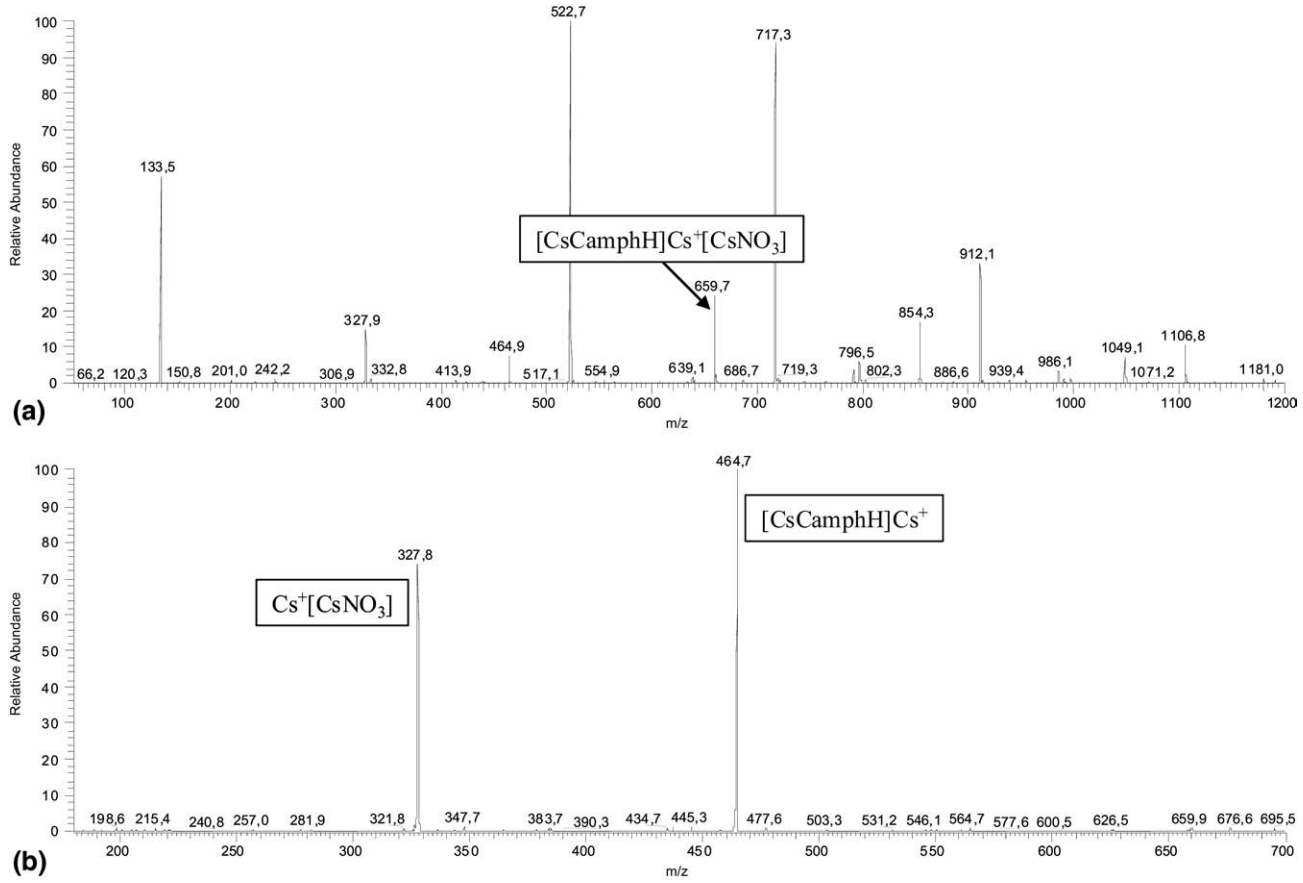

Figure 2. (**a**) Electrospray mass spectrum of a methanol/water solution containing camphoric acid and cesium nitrate. The majority of ions correspond to $[Cs^+[Cs^+NO_3^-]_n]^+$ and $[Cs^+[Cs^+NO_3^-]_n[Cs^+CamphH^-]_m]^+$ with $CamphH^-$ = hydrogen camphorate ion; (**b**) CID spectrum of the $[Cs^+[Cs^+NO_3^-][Cs^+CamphH^-]]^+$ ion.

(reference of similar structure), both situations fulfilling the condition $\Delta\Delta S \approx 0$. More details on the limitation and breadth of the kinetic method can be found in reference [44].

The application of the kinetic method using the standardized conditions described in the experimental part provides three relative scales. The results obtained for the branching ratio of the dissociation of the cesium bound dimers $[CsX]Cs^+[CsA]$ ($X^- = NO_3^-$, I^-, CF_3COO^-; A^- = carboxylate) into $Cs^+[CsX]$ and $Cs^+[CsA]$ are reported in Table 2.

Owing to the good dynamic range of the CID spectra, the $\ln(I/I_0)$ scale reaches almost 10 units. The uncertainties tend to increase when the absolute values of $\ln(I/I_0)$ are large, i.e., when one of the ions exhibits a weak intensity and a low signal/noise ratio. Specific experimental difficulties (low signal intensity of a particular cluster, reproducibility of the intensity ratios, secondary dissociation products) limit also the precision in a few cases. The worst precisions are observed for the measurements on cesium hydrogen trans-aconitate and hydrogen tricarballylate. In these cases, we observed the neutral loss of HNO_3, giving an ion containing three Cs atoms and a doubly charged anion A^{2-}, $Cs^+[Cs_2A]$. The result of this concurrent dissociation is a weak intensity for the two expected ions of Scheme **2**, and a loss of repeatability. In fact, for total variations of $\ln(I/I_0)$ scales of about 10 ln units, most uncertainties are in the range 0.03–0.4.

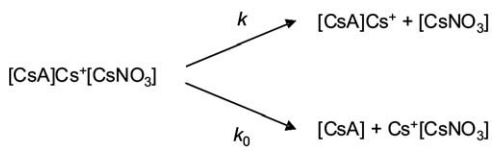

Scheme 2. Application of the kinetic method to the dissociation of a simple Cs^+ mixed cluster with cesium nitrate and a series of cesium carboxylate.

From data in Table 2, we can compare the three $\ln(I/I_0)$ scales for 10 cesium carboxylates. In Figure 3, $\ln(I/I_0)$ values relative to [CsTFA] and [CsI] were plotted against the values relative to $[CsNO_3]$.

A good linearity is observed, with slopes close to unity (see statistical parameters in caption of Figure 3), showing that the kinetic method gives consistent results independently from the reference salt. The relative affinities are not significantly dependent of the structure of the reference salt. The slopes in eqs 2 and 3 are

Table 2. Experimental branching ratio $\ln(I/I_0)$ for the dissociation of the cesium bound dimers $[CsX]Cs^+[CsA]$ ($X^- = NO_3^-$, I^-, CF_3COO^-; A^- = cesium carboxylate) into $Cs^+[CsX]$ and $Cs^+[CsA]$. Each value is the mean of about 15 measurements and uncertainties are the corresponding standard deviations. Column 5 contains the CsCA values (based on $[CsNO_3]$) evaluated from the correlation equations given in Figure 3, except when values for [CsI] and [CsTFA] salts are not available. Column 6 contains the CsCA values based on $\ln(I/I_0)$ of column 5, using eq 4

A–[a]	$[CsNO_3]$	[CsI]	[CsTFA]	$[CsNO_3]$[b]	CsCA
Hydrogen dimethylmalonate	4.30 ± 0.22			4.30	171.0
Hydrogen trans-aconitate	4.15 ± 1.64			4.15	170.1
Hydrogen cis-aconitate	3.34 ± 0.43			3.34	165.0
Hydrogen malonate	3.27 ± 0.23[c]			3.27	164.6
3-Benzoyl propionate	3.26 ± 0.09	4.68 ± 0.25	7.18 ± 0.33	3.20	164.2
Hydrogen tricarballylate	3.17 ± 1.37			3.17	163.9
Hydrogen phthalate	2.94 ± 0.05[c]			2.94	162.5
Hydrogen ketoglutarate		4.24 ± 0.20		2.78	161.5
Hydrogen homophthalate		4.21 ± 0.49		2.76	161.4
Hydrogen maleate	2.19 ± 0.25[c]	4.60 ± 0.16		2.65	160.7
Hydrogen succinate	2.38 ± 0.05	4.34 ± 0.20		2.63	160.6
Hydrogen methylsuccinate	2.38 ± 0.16			2.38	159.0
Hydrogen citrate	1.85 ± 0.61			1.85	155.7
Hydrogen oxalate	0.36 ± 0.18[c]	2.24 ± 0.07	5.30 ± 0.34	0.83	149.4
Hydrogen glutarate	0.68 ± 0.03	1.90 ± 0.05		0.65	148.2
Hydrogen camphorate	0.51 ± 0.14	1.65 ± 0.06		0.45	146.9
Hydrogen adipate	0.43 ± 0.03	1.40 ± 0.03	4.19 ± 0.11	0.21	145.5
Hydrogen methyladipate	0.19 ± 0.16			0.19	145.4
4-Aminobenzoate		1.27 ± 0.03[d]		0.03	144.3
Hydrogen tartrate	−0.97 ± 0.21	−0.01 ± 0.29	3.42 ± 0.68	−0.96	138.2
4-Methylbenzoate		−0.33 ± 0.09[d]		−1.45	135.1
Hydrogen 2-hydroxysuccinate	−1.46 ± 0.02	−0.31 ± 0.05	2.28 ± 0.16	−1.61	134.1
3-Methylbenzoate		−0.65 ± 0.05[d]	2.29 ± 0.03	−1.75	133.2
Glycolate	−2.20 ± 0.07	−1.09 ± 0.09	2.33 ± 0.07	−2.08	131.1
Gallate		−1.18 ± 0.06		−2.25	130.1[e]
3-Hydroxybenzoate		−1.93 ± 0.09[d]		−2.94	125.8[e]
Benzoate	−2.93 ± 0.20	−1.79 ± 0.15[d]	1.12 ± 0.04	−2.96	125.7
Trans-cinnamate	−2.76 ± 0.11	−1.92 ± 0.05	0.89 ± 0.05	−3.02	125.3
3-Nitrobenzoate		−2.39 ± 0.18[d]		−3.37	123.1[e]
4-Hydroxybenzoate		−2.48 ± 0.12[d]		−3.46	122.6[e]
4-Nitrobenzoate		−3.13 ± 0.12[d]		−4.05	118.8[e]
Hydrogen fumarate	−5.19 ± 0.36[c]	−4.73 ± 0.43	−0.68 ± 0.17	−5.24	111.4
Salicylate	−6.36 ± 0.58[c]	−5.29 ± 0.39	−1.86 ± 0.04	−6.22	105.3

[a]Structure of the acid given on Scheme **1**.
[b]Experimental value or from correlations in caption of Figure 3; see text for the method of estimation and uncertainties.
[c][27].
[d][28].
[e]The added Cs^+ may not be bound at the carboxylate group.

related to the effective temperature T_{eff}, so the slope for the plots in Figure 3 means that T_{eff} values are almost identical for the three series, indicating very similar conditions of collisional activation.

For establishing the most complete possible scale of relative Cs^+ basicities, in term of $\ln(I/I_0)$, the values lacking for $[CsNO_3]$ as reference were estimated from the two equations given in Figure 3 and experimental values for [CsTFA] and [CsI] in Table 2. When more than one value can be estimated through this procedure, the mean value is reported in the last column of Table 2. Uncertainties on these estimated $\ln(I/I_0)$ values are difficult to assess consistently, because they are either direct experimental values, estimated from one or two calculated values, or a mix of the three. A more comprehensive estimation can be made by examining the standard deviations of 0.32 and 0.45 units for the regression equations of Figure 3. This uncertainty range is consistent with the mean reproducibility of $\ln(I/I_0)$ values. The data in the fifth column of Table 2 represent a relative affinity (or basicity) scale relative to Cs^+. However, to be of more general usefulness, the $\ln(I/I_0)$ values must be scaled and anchored to absolute values. As there is no experimental data for such purpose, the scaling and anchoring process can be done by using absolute CsCA or CsCB values calculated by quantum chemistry.

Calibration of the ln(I/I$_0$) with DFT Values

Many organic acids in Scheme **1** (and especially their cesium cation adducts), having thousands of possible conformations, are conformationally too flexible, so the DFT calculations were performed on a subset of 18 simple compounds listed in Table 3. Although the choice was partly arbitrary, it was a compromise be-

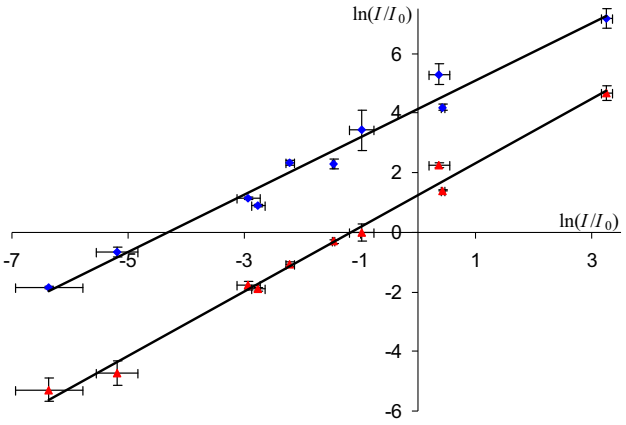

Figure 3. Plot of $\ln(I/I_0)$ referenced to [CsTFA] (filled diamond) and [CsI] (filled triangle) versus the values for [$CsNO_3$]. Parameters of the regression equations (r^2 = squared correlation coefficient; s and uncertainties are standard deviations): (filled diamond) y = (0.963 ± 0.053) x + (4.13 ± 0.17); s = 0.45; r^2 = 0.9763/(filled triangle) y = (1.077 ± 0.038) x + (1.24 ± 0.12), s = 0.32; r^2 = 0.9902.

tween the structural diversity and the complexity of calculations.

The final geometries of the salts [CsA] and their adducts Cs^+[CsA] correspond to the optimization steps: (1) anion(s) geometry and possible tautomers, (2) salt(s) geometries, (3) geometries of the Cs^+ adduct of the salt(s). For the salts and adducts, different initial positions of the cations were tried. The most stable geometries for calculated systems are illustrated in the Supplementary Material, and their corresponding thermodynamic functions H and G are given. When optimizing Cs^+[CsA] geometries produces very close energies, the corresponding structures are also shown. The structural effects on cesium cation affinities (CsCA) are discussed in the next section.

The structures of the molecular salt [Cs^+A^-] are relatively straightforward. The cesium cation interacts with the two oxygen atoms of the carboxylate anion, with two nearly equal Cs^+–O distances and Cs^+ sitting in the plane of the carboxylate group.

The adducts Cs^+[CsA] may assume different structures of relatively close enthalpies or Gibbs free energies. The adducts of monocarboxylic acid salts are considered first. In the case of 3- and 4-substituted benzoates [28], the different conformations assumed by the salt adduct Cs^+[CsA] have been described in detail. For benzoates with substituent(s) in positions 3 and 4 included in the present study, two situations should be considered. When the substituent does not bind strongly Cs^+, as for NH_2 and OH, and for the unsubstituted benzoate, two conformations of the adduct show close energy minimums, and accordingly close CsCA (or CsCB) values. In one form, the two Cs^+ are located approximately in the direction of the two C–O bonds of the carboxylate group (see Scheme 3, Form A).

The second form resembles the initial salt with the additional Cs^+ above the plane of the carboxylate, close to one of the oxygen atom and leaning toward the benzene ring (Form B). This is reminiscent to the cation/π interaction [45], which was observed in several adducts of alkali metal cation with neutral aromatic molecules [46, 47], in particular when the benzene ring carries an electron rich substituent. The trans-cinnamate adduct behaves similarly, giving a B-type adduct with the additional Cs^+ being oriented toward the ethylenic bond. Typically, the calculated CsCA values corresponding to the two Forms A and B are within 0.4–7 kJ/mol. The situation for the 3- and 4-nitrobenzoates adducts is different because the most stable structures correspond to the second cesium cation bound to the NO_2 group [28].

In the gas phase, the 4-hydroxybenzoic acid is a stronger acid at the OH than at the COOH [48], but the reverse is true in water and methanol [28]. In our ESI studies, the carboxyl group, which is the most acidic in solution, may remain in the anionic state (and bound to Cs^+) during the desolvation process. In fact, the experimental study of substituted benzoates indicated that the 3- and 4-hydroxybenzoates did not behave exactly as the other members of the series [28]. Possibly the anionic site shifted to the phenolic group in the ESI process. As the present work focuses on carboxylate salts, calculations involving the 3- and 4-hydroxybenzoates in the form of phenolate salts were disregarded. The stable form of the 2-hydroxybenzoate (salicylate anion and the corresponding salt) corresponds to a carboxylate stabilized by an internal hydrogen bond. The cesium salt of 2-hydroxyacetic (glycolic) acid exhibits a similar stabilization in the molecular salt. In the Cs^+ adduct, the

Table 3. Calculated (DFT B3LYP/D95V+ (d,p)/SDD*) enthalpies (CsCAs) (kJ/mol at 298 K) for the dissociation of Cs^+[CsA] into Cs^+ and [CsA] (Corresponding Gibbs free energies, CsCB, and entropies are given as Supplementary Material)

A^- in [Cs^+A^-]	CsCA
Hydrogen phthalate	171.7
Hydrogen dimethylmalonate	167.4
Hydrogen maleate	164.5
Hydrogen malonate	161.5
Hydrogen oxalate	142.4
4-Aminobenzoate	137.6
Glycolate	136.3
Gallate[a]	133.4
3-Hydroxybenzoate[a]	127.9
4-Methylbenzoate	129.2
3-Methylbenzoate	129.2
4-Hydroxybenzoate[a]	127.3
Trans-cinnamate	127.1
Benzoate	125.1
3-Nitrobenzoate[b]	120.5
4-Nitrobenzoate[b]	119.5
Hydrogen fumarate	115.5
Salicylate	112.1

[a]The value correspond to the cesium carboxylate tautomer (as opposed to the phenolate, see text).
[b]The value corresponds to the adduct with the added Cs^+ bound to the nitro group (most stable complex).

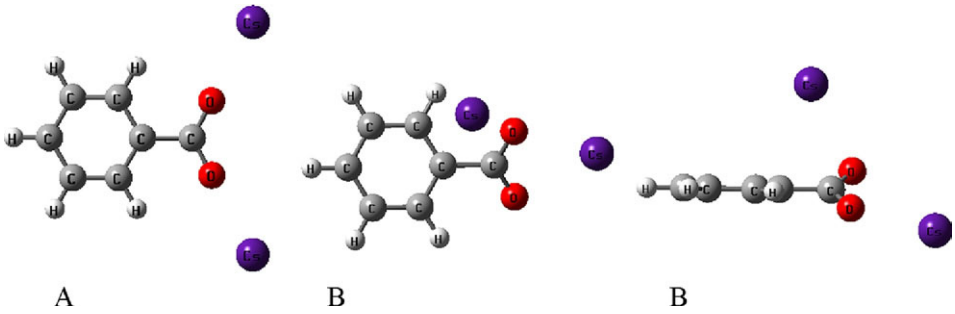

Scheme 3. Two most stables conformations (calculated lowest *H* function) of the Cs^+ adduct of cesium benzoate (form B seen from two different directions).

cesium glycolate binds the additional cation by two oxygen atoms: one from the carboxylate and the other from hydroxyl. In this adduct, as opposed to the salicylate case, the hydrogen bond is broken.

Calculations were also carried out on salts of diacid monoanions. To avoid too much conformational complexity, the smallest systems or the most rigid structures were considered. These situations correspond to relatively close carboxyl groups in position such that they can interact by a hydrogen bond. In the monoanion, a hydrogen bond between the carboxylate and the carboxyl group serve to transfer a part of the negative charge of the anionic part to the neutral group, as shown in Scheme 4. This group presents therefore a favorable site for bonding the second Cs^+.

The oxalate salt and its adduct display structures that are different from those generated from other diacids (see Supplementary Material). In the most stable form of the cesium oxalate, the cation is situated between the two carboxyl groups. In the corresponding stable adduct, the second Cs^+ is preferentially bound to the two oxygen atoms of one of the carboxyl.

In the following discussion, only the largest CsCA values, corresponding to the most stable structures, are retained for our purpose, and are listed in Table 3 (CsCB and entropy are available as Supplemental Data to Table 3; *H* and *G* parameters for other geometries close in energy are given in the Supplementary Material).

The application of the kinetic method is justifiable if we consider that the bonding between Cs^+ and the different cesium carboxylates is reasonably analogous. The bonding in the dissociating dimer and in the adduct should be also relatively similar. The constant entropy condition (see calculated entropies in Supplemental Data for Table 3) was also implied for the application of eqs 2 and 3. Under these conditions, a linear relationship between the $\ln(I/I_0)$ and CsCA (or CsCB) values is expected. However, for reasons discussed above, there is some doubt about the exact site of Cs^+ bonding for the anions of the following benzoic acids: 3- and 4-OH, gallic (3,4,5-trihydroxy), 3- and 4-NO_2, and the corresponding data were excluded from the statistical analysis. This plot, involving the remaining 13 $\ln(I/I_0)$ values linked to cesium nitrate (Table 2, penultimate column) versus DFT-calculated CsCA is shown on Figure 4.

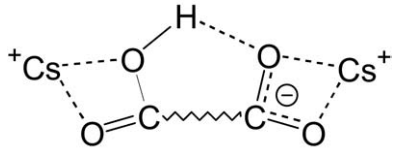

Scheme 4. Hydrogen bonding interaction within the monoanion of a dicarboxylic acid promoting the bonding of two Cs^+.

For these 13 points, the corresponding statistics (r^2 = squared correlation coefficient or coefficient of determination; *s* and uncertainties = standard deviations; CsCA in kJ/mol) are:

$$\ln(I/I_0) = (0.160 \pm 0.013)\text{CsCA} - (23.07 \pm 1.855);$$
$$s = 0.91;\ r^2 = 0.9310 \qquad (4)$$

From the slope, the effective temperature is T_{eff} = (751 ± 61) K. This is in close agreement with previous measurements on a more limited series [27]. A correlation with CsCB (not shown; see Supplemental Data for Table 2) is very similar. From the structural point of

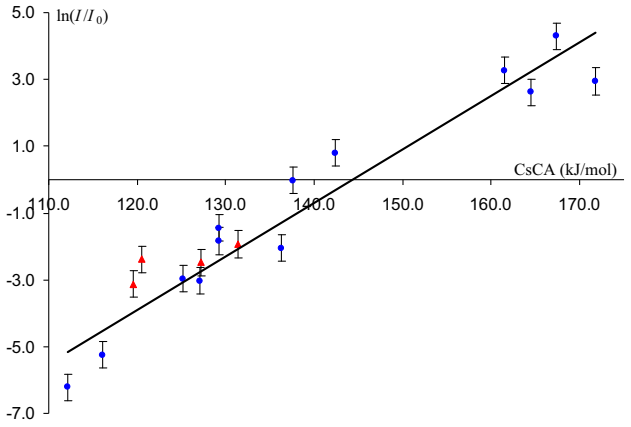

Figure 4. Plot of $\ln(I/I_0)$ (logarithms of the branching ratios for the dissociation of $[Cs^+NO_3^-][Cs^+[Cs^+A^-]$, see Scheme 2) (filled circle) versus DFT calculated enthalpies of dissociation of $Cs^+[Cs^+A^-]$ (CsCA) (filled triangle]). Data not included in the statistical analysis. The marked uncertainties on $\ln(I/I_0)$ are set to ±0.4 units.

view, the series of cesium benzoates [28] was more homogeneous than the present series, at the cost of restricted range of CsCA, with a slightly better precision and a higher slope ($T_{eff} \approx 500$ K). Despite the uncertainty about the site of interaction of Cs^+, the five data that were excluded from the correlation appear to fit the linear relationship. For the 3- and 4-NO_2 benzoates, we suggest that the nitro group behaves similarly to a carboxylate for Cs^+ bonding, and consequently fulfill the criteria for the applicability of kinetic method within our series. For the data involving 3- and 4-hydroxybenzoic acids, the deviations from the kinetic plot previously observed [28] are not obvious here. The process of rescaling to the common reference [$CsNO_3$] (experiments run with [CsI]) apparently smoothes away the specific deviations observed in the benzoate series. The 3,4,5-trihydroxy benzoate (gallate) is expected to behave like the 3- and 4-hydroxy compounds, and indeed follows also the linear trend. Overall, there is no strong evidence that in the ESI process, hydroxybenzoic acids generate phenolate anions and salts instead of carboxylates. DFT calculations on 3- and 4-hydroxybenzoic acids and gallic acid also confirm that the carboxylate form of cesium adducts is always more stable in gas phase, possibly due to the ability of cesium cation to interact simultaneously with both oxygens of the carboxylate group.

Using eq 4, $\ln(I/I_0)$ can be converted into CsCA. Although these values are adjusted on theoretical grounds, it is obvious that they are established experimentally. For 33 molecular salts, the CsCA scale covers 66 kJ/mol. The largest error on $\ln(I/I_0)$ (± 1.64 occurring for hydrogen trans-aconitate) translates into about ± 10 kJ/mol, but most uncertainties are in the range 0.2–3 kJ/mol. The standard errors on slope and intercepts of eq 4 are not included in this uncertainty evaluation, as we considered they are simple scaling parameters that may be improved by enhancing the computation level. The resulting scale of cesium cation affinity (CsCA) of the molecular salt [CsA] are collected in the last column of Table 2. The CsCA values constitute a new kind of affinity scale. When the sites of interaction of the second Cs^+ is uncertain, as indicated by calculated most stable structures, it may be unsound to apply the kinetic method, and the corresponding values are given a note of caution in Table 2.

Structural Effects on the Cesium Cation Affinity of Carboxylate Salts

A global observation of the CsCA values listed in Table 2 is that the monoacid salts are generally weaker bases than the di- and triacid salts. One obvious reason for the higher CsCA of the diacids salts can be deduced from the calculated structures of the adducts: the distance between the two cations minimize the Coulomb repulsion. One exception is 3-benzoyl propionate, which displays an affinity larger than for the other monoacid salts. The carbonyl group may assist the bonding of the additional Cs^+ by chelate formation.

The order of decreasing CsCA for aliphatic diacids salts is (hydrogen is omitted in the name of the monoanion): malonate > succinate > (oxalate) > glutarate > adipate. Except for oxalate, this sequence is exactly the order of increasing number of carbons between the carboxyl groups. The hydrogen malonate has the most favorable carbon skeleton to form an optimal hydrogen bond, within a six-membered ring, as shown in Scheme 4. As explained before, the structure of the adduct of cesium hydrogen oxalate departs from that of the other diacid salts adducts. The relative orientation of the two carboxyl functions turns up to be essential for an enhanced bonding of the second Cs^+, like with maleic and phthalic acids salts, for which the rigid framework appears to promote this bonding characteristic. Compared with phthalic acid, the conformational freedom of one of the carboxyl group in the homophthalic acid does not change significantly the CsCA value. The geometry constraint in the camphoric acid, for which the two carboxyl groups are *cis*, does not induce a significant difference with the salt of glutaric acid, which has the same number of carbon atoms between the carboxyl groups, and is not conformationally constrained. The same observation can be done for the salts of maleic and succinic acids, which are close in CsCA, despite the differences in conformational freedom. On the other hand, the rigid *trans* structure of fumaric acid hampers the interaction between the acid functions. Consequently, cesium hydrogen fumarate behaves like a monoacid salt and presents a correspondingly low CsCA. Considering the number of possible deprotonation sites, the number of conformations of the anion and the multiplicity of the interaction sites with the cesium cation, triacids were not studied computationally. The CsCA values of the triacid salts are in decreasing order (acid name given): trans-aconitic > cis-aconitic > tricarballylic > citric, and are in the range of those of the diacid salts. The absence of strong geometrical effects observed for the diacids salts appears to be valid for the triacids salts. The presence of a third carboxylic function (for example, compare salts of maleic or succinic and *cis*-aconitic; succinic, and tricarballylic) does not generate a CsCA increase.

The presence of substituents on the carbon skeleton may also affect the CsCA values of the salts. From calculated and experimental CsCA in the cesium benzoate series bearing meta and para substituents [28], the electron releasing or withdrawing effects [49] produce respectively the anticipated CsCA increase or decrease. Adding methyl substituents on alkyl chains is expected to increase CsCA by polarizability effects [49]. Such effect occurs in the case of dimethyl malonic salt, but it is negligible, and actually in the wrong direction, for the methyl effect in succinate and adipate. The small methyl polarizability effect may be offset by hindrance to the optimal hydrogen bond interaction that induces the high CsCA values of these diacids. Substitution by

hydroxyl groups produces a decrease in CsCA in the case of diacid salts, as observed for 2-hydroxysuccinate and tartaric versus succinate. To some extent, this may be due to the electron withdrawing field/inductive effect of the OH group. In addition, the formation of a hydrogen bond between the hydroxyl and the carboxyl or carboxylate groups in salts of the diacids studied decreases the electron density at the cation-bonding site and weaken the basicity. In the case of triacid salts, the decrease of CsCA induced by the hydroxyl group (tricarballylic versus citric) is much more modest. Likely the third carboxyl group is favored as hydrogen bond donor relative to the hydroxyl, resulting in a situation close to that described for diacid salts (Scheme 4).

Conclusions and Perspectives

Electrospray ionization of mixtures of a cesium salt (either nitrate, iodide, or trifluoroacetate, considered as reference salts) and a carboxylic acid produces positively charged clusters containing essentially cesium salt units (reference salt and/or carboxylates) bound to a cesium cation. The simplest mixed cluster contains the reference salt and a cesium carboxylate bound by a cesium cation. CID of this mixed cluster generates cesium adducts of the reference salt $[CsX]Cs^+$ and of the carboxylate $[CsRCOO]Cs^+$. Energetics of the cesium cation bonding to the molecular salt can be characterized by application of the kinetic method to the CID data. By combining these data and results of DFT calculations, a quantitative cesium cation affinity (CsCA) scale for the molecular carboxylate was developed. The present work represents a new approach of the characterization of the interaction between Cs^+ and the carboxylate function. To our knowledge, our experimental and theoretical studies on the energetics of Cs^+/[CsA] interaction are the first characterization of gas-phase molecular salts [CsA] as Lewis bases. Depending on the structure, the addition of the second cesium cation on cesium carboxylate salts occurs in different ways. Monoacids salts bind the additional Cs^+ at the carboxylate function in such a way that each cation in $[CsRCOO]Cs^+$ is bound to one of the two oxygen atoms of the carboxylate, minimizing Coulomb repulsion. In the case of aromatic monoacid salts, the additional Cs^+ tends to be located toward the benzene ring, indicating some additional stabilization of these adducts by cation/π interaction. The salts of the di- and tricarboxylic acids exhibit larger Cs^+ affinities than monoacids, when the geometry of the framework allows the two acid functions to come close enough. This increased CsCA is attributed to a hydrogen bonding interaction between the hydrogen bond donor COOH and the hydrogen bond acceptor COO^-, which permit the two cations to be bound on two different functions and to release the Coulomb repulsion.

We are currently exploring two points that may strengthen and enlarge the proposed CsCA scale: (1) verification of relative affinities (or basicities) by using clusters formed with two carboxylate salts $[CsRCOO]Cs^+[CsR'COO]$; direct comparisons between structurally related salts may lead to better fulfillment of condition for applying the kinetic method; (2) the entropy effects using the extended kinetic method [50] not used here because of instrumental limitations.

Other possibilities are also considered to further increase our knowledge of the interaction between acidic organic molecules and Cs^+ in the context of transport of cesium by humic substances. Studies of Cs^+ adducts formation with polymeric (or oligomeric) acids that mimic behavior of fulvic acids toward cation (Cs^+), like polyacrylic acid, are currently carried out. Finally, the intrinsic Cs^+/carboxylate anion interactions would be of primary interest for our purpose. We are investigating the energetics of these systems by the application of the kinetic method to negatively charged clusters $[A^-Cs^+A'^-]$.

Acknowledgments

C.M. thanks the French Ministry of Research for scholarship. Part of the quantum calculations were carried out in the framework of the Estonian Science Foundation exchange program Archimedes. Professor Laurence Charles (Marseille) is gratefully acknowledged for preliminary experiments on the QTOF instrument of the Mass Spectrometry facility. The authors thank Sanofi-Aventis for the gift of two ion trap mass spectrometers (Thermo LCQ) to the Mass Spectrometry facility of the University of Nice-Sophia Antipolis, and are indebted to Mr. F. Jaulin (Sanofi-Aventis France) for his collaboration.

Appendix A Supplementary Material

Supplementary material associated with this article may be found in the online version at doi:10.1016/j.jasms.2009.07.003.

References

1. Unterweger, M. P.; Hoppes, D. D.; Schima, F. J. New and Revised Half-Life Measurements Results. *Nucl. Instrum. Methods Phys. Res. A* **1992,** *312*, 349–352; Unterweger, M. P. Radionuclide Half-Life Measurements (version 3.0, April 2003). Available online: http://physics.nist.gov/Halflife. National Institute of Standards and Technology: Gaithersburg, MD, USA.
2. Pourcelot, L.; Louvat, D.; Gauthier-Lafaye, F.; Stille, P. Formation of Radioactivity Enriched Soils in Mountain Areas. *J. Environ. Radioact.* **2003,** *68*, 215–233.
3. Zhiyanski, M.; Sokolovska, M.; Lucot, E.; Badot, P.-M. Cs-137 Contamination in Forest Ecosystems in Southwest Rila Mountain, Bulgaria. *Environ. Chem. Lett.* **2005,** *3*, 49–52.
4. Rezzoug, S.; Michel, H.; Fernex, F.; Barci-Funel, G.; Barci, V. Evaluation of ^{137}Cs Fallout from the Chernobyl Accident in a Forest Soil and its Impact on Alpine Lake Sediments, Mercantour Massif, S.E. France. *J. Environ. Radioact.* **2006,** *85*, 369–379.
5. (a) Garaudée, S.; Elhabiri, M.; Kalny, D.; Robiolle, C.; Trendel, J.-M.; Hueber, R.; Van Dorsselaer, A.; Albrecht, P.; Albrecht-Gary, A.-M. Allosteric Effects in Norbadione A. A Clue for the Accumulation Process of ^{137}Cs in Mushrooms? *Chem. Commun.* **2002,** *944-945;* (b) Desage-El Murr, M.; Nowaczyk, S.; Le Gall, T.; Mioskowski, C.; Amekraz, B.; Moulin, C. Norbadione A: Synthetic Approach to the Bis(pulvinic acid) Moiety and Cesium Complexation Studies. *Angew. Chem. Int. Ed.* **2003,** *45*, 1289–1293; (c) Giovani, C.; Garavaglia, M.; Scruzzi, E. Radiocaesium in Mushrooms from Northeast Italy, 1986–2002. *Radiat. Prot. Dosimetry* **2004,** *111*, 377–383; (d) Tadaaki Ban-nai, T.; Yoshida, S.; Muramatsu, Y.; Akira Suzuki, A. Uptake of Radiocesium by Hypha of Basidiomycetes-Radiotracer Experiments. *J. Nucl. Radiochem. Sci.* **2005,** *6*, 111–113; (e) Karadeniz, O.; Yaprak, G. Dynamic Equilibrium

of Radiocesium with Stable Cesium Within the Soil-Mushroom System in Turkish Pine Forest. *Environ. Pollut.* **2007,** *148*, 316–324.
6. Su, Y.; Maruthi Sridhar, B. B.; Han, F. X.; Diehl, S. V.; Monts, D. L. Effect of Bioaccumulation of Cs and Sr Natural Isotopes on Foliar Structure and Plant Spectral Reflectance of Indian Mustard (Brassica Juncea). *Water Air Soil. Pollut.* **2007,** *180*, 65–74.
7. Paller, M. H.; Jannik, G. T.; Fledderman, P. D. Changes in ^{137}Cs Concentrations in Soil and Vegetation on the Floodplain of the Savannah River over a 30 Year Period. *J. Environ. Radioact.* **2008,** *99*, 1302–1310.
8. (a) Hurel, C.; Marmier, N.; Séby, F.; Giffaut, E.; Bourg, A. C. M.; Fromage, F. Sorption Behavior of Caesium on a Bentonite Sample. *Radiochim. Acta* **2002,** *90*, 695–698; (b) Hurel, C.; Marmier, N.; Bourg, A. C. M.; Fromage, F. Sorption of Cs and Rb on Purified and Crude MX-80 Bentonite in Various Electrolytes. *J. Radioanal. Nucl. Chem.* **2009,** *279*, 113–119.
9. Dumat, C.; Staunton, S. Reduced Adsorption of Caesium on Clay Minerals Caused by Various Humic Substances. *J. Environ. Radioact.* **1999,** *46*, 187–200.
10. Staunton, S.; Dumat, C.; Zsolnay, A. Possible Role of Organic Matter in Radiocaesium Adsorption in Soils. *J. Environ. Radioact.* **2002,** *58*, 163–173.
11. Nakamaru, Y.; Ishikawa, N.; Tagami, K.; Uchida, S. Role of Soil Organic Matter in the Mobility of Radiocesium in Agricultural Soils Common in Japan. *Colloids Surf. A Physicochem. Eng. Asp.* **2007,** *306*, 111–117.
12. Sutton, R.; Sposito, G. Molecular Structure in Soil Humic Substances: The New View. *Environ. Sci. Technol.* **2005,** *39*, 9009–9015.
13. McCarthy, P. The Principles of Humic Substances. *Soil Sci.* **2001,** *166*, 738–751.
14. Albers, C. N.; Banta, G. T.; Jacobsen, O. S.; Hansen, P. E. Characterization and Structural Modeling of Humic Substances in Field Soil Displaying Significant Differences from Previously Proposed Structures. *Eur. J. Soil. Sci.* **2008,** *59*, 693–705.
15. Tipping, E. Cation Binding by Humic Substances, 1st ed. In *Cambridge Environmental Chemistry*, Vol. XII, Chap. 8; Cambridge University Press: Cambridge, UK, 2002.
16. Cardoza, L. A.; Korir, A. K.; Otto, W. H.; Wurrey, C. J.; Larive, C. K. Application of NMR Spectroscopy in Environmental Science. *Prog. Nucl. Magn. Reson. Spectrosc.* **2004,** *45*, 209–238.
17. Christl, I.; Milne, C. J.; Kinniburgh, D. G.; Kretzschmar, R. Relating Ion Binding by Fulvic and Humic Acids to Chemical Composition and Molecular Size. II. Metal Binding. *Environ. Sci. Technol.* **2001,** *35*, 2512–2517.
18. Leenheer, J. A.; Brown, G. K.; MacCarthy, P.; Cabaniss, S. E. Models of Metal Binding Structures in Fulvic Acid from the Suwannee River, Georgia. *Environ. Sci. Technol.* **1998,** *32*, 2410–2416.
19. Baziramakenga, R.; Simard, R. R.; Leroux, G. D. Determination of Organic Acids in Soil Extracts by Ion Chromatography. *Soil. Biol. Biochem.* **1995,** *27*, 349–356.
20. Strobel, B. W. Influence of Vegetation on Low-Molecular-Weight Carboxylic Acids in Soil—a Review. *Geoderma* **2001,** *99*, 169–198.
21. (a) Ehlken, S.; Kirchner, G. Environmental Processes Affecting Plant Root Uptake of Radioactive Trace Elements and Variability of Transfer Factor Data: A Review. *J. Environ. Radioact.* **2002,** *58*, 97–112; (b) Degryse, F.; Verma, V. K.; Smolders, E. Mobilization of Cu and Zn by Root Exudates of Dicotyledonous Plants in Resin-Buffered Solutions and in Soil. *Plant Soil* **2008,** *306*, 69–84.
22. (a) Krivacsy, Z.; Kiss, G.; Varga, B.; Galambos, I.; Sarvari, Z.; Gelencser, A.; Molnar, A.; Fuzzi, S.; Facchini, M. C.; Zappoli, S.; Andracchio, A.; Alsberg, T.; Hansson, H. C.; Persson, L. Study of Humic-Like Substances in Fog and Interstitial Aerosol by Size-Exclusion Chromatography and Capillary Electrophoresis. *Atm. Environ.* **2000,** *34*, 4273–4281; (b) Kiss, G.; Varga, B.; Gelencser, A.; Krivacsy, Z.; Molnar, A.; Alsberg, T.; Persson, L.; Hansson, H.-C.; Facchini, M. C. Characterization of Polar Organic Compounds in Fog Water. *Atm. Environ.* **2001,** 35, 2193–2200.
23. Kippenberger, M.; Winterhalter, R.; Moortgat, G. K. Determination of Higher Carboxylic Acids in Snow Samples Using Solid-Phase Extraction and LC/MS-TOF. *Anal. Bioanal. Chem.* **2008,** *392*, 1459–1470.
24. Smith, J. N.; Rathbone, G. J. Carboxylic Acid Characterization in Nanoparticles by Thermal Desorption Chemical Ionization Mass Spectrometry. *Int. J. Mass Spectrom.* **2008,** *274*, 8–13.
25. Gal, J.-F.; Maria, P.-C.; Massi, L.; Mayeux, C.; Burk, P.; Tammiku-Taul, J. Cesium Cation Affinities and Basicities. *Int. J. Mass Spectrom.* **2007,** *267*, 7–23.
26. Maria, P.-C.; Gal, J.-F.; Massi, L.; Burk, P.; Tammiku-Taul, J.; Tamp, S. Investigation of Cluster Ions Formed Between Cesium Cations and Benzoic, Salicylic and Phthalic Acids by Electrospray Mass Spectrometry and Density-Functional Theory Calculations. Toward a Modeling of the Interaction of Cs^+ with Humic Substances. *Rapid Commun. Mass Spectrom.* **2005,** *19*, 568–573.
27. Maria, P.-C.; Massi, L.; Sindreu Box, N.; Gal, J.-F.; Burk, P.; Tammiku-Taul, J.; Kutsar, M. Bonding Energetics in Clusters Formed by Cesium Salts: A Study by Collision-Induced Dissociation and Density Functional Theory. *Rapid Commun. Mass Spectrom.* **2006,** *20*, 2057–2062.
28. Mayeux, C.; Massi, L.; Gal, J.-F.; Maria, P.-C.; Tammiku-Taul, J.; Lohu, E.-L.; Burk, P. Bonding Between Cesium Cation and Substituted Benzoic Acids or their Anions in the Gas Phase: Density Functional Theory and Mass Spectrometry Study. *Collect. Czech. Chem. Commun.* **2009,** *74*, 167–188.
29. (a) Cooks, R. G.; Kruger, T. L. Intrinsic Basicity Determination Using Metastable Ions. *J. Am. Chem. Soc.* **1977,** *99*, 1279–1281; (b) Cooks, R. G.; Patrick, J. S.; Kotiaho, T.; McLuckey, S. A. Thermochemical Determinations by the Kinetic Method. *Mass Spectrom. Rev.* **1994,** *13*, 287–339. (c) Cooks, R. G.; Wong, P. S. H. Kinetic Method of Making Thermochemical Determinations: Advances and Applications. *Acc. Chem. Res.* **1998,** *31*, 379–386.
30. (a) Chen, G.; Cooks, R. G. Estimation of Heterolytic Bond Dissociation Energies by the Kinetic Method. *J. Mass Spectrom.* **1997,** *32*, 1258–1261; (b) Wu, L.; Denault, J. W.; Cooks, R. G.; Drahos, L.; Vékey, K. Alkali Chloride Cluster Ion Dissociation Examined by Kinetic Method: Heterolytic Bond Dissociation Energies, Effective Temperatures, and Entropic Effects. *J. Am. Soc. Mass Spectrom.* **2002,** *13*, 1388–1395.
31. McIntyre, C.; McRae, C. Proposed Guidelines for Sample Preparation and ESI-MS Analysis of Humic Substances to Avoid Self-Esterification. *Org. Geochem.* **2005,** *36*, 543–553.
32. McIntyre, C.; McRae, C.; Jardine, D.; Batts, B. D. Self-Esterification of Fulvic Acid Model Compounds in Methanolic Solvents as Observed by Electrospray Ionization Mass Spectrometry. *Rapid Commun. Mass Spectrom.* **2002,** *16*, 785–789.
33. McClellan, J. E.; Phy, J.; Mulholland, J. J.; Yost, R. A. Effects of Fragile Ions on Mass Resolution and on Isolation for Tandem Mass Spectrometry in the Quadrupole Ion Trap Mass Spectrometer. *Anal. Chem.* **2002,** *74*, 402–412.
34. Frisch, M. J.; Trucks, G. W.; Schlegel, H. B.; Scuseria, G. E.; Robb, M. A.; Cheeseman, J. R.; Montgomery, J. A. Jr.; Vreven, T.; Kudin, K. N.; Burant, J. C.; Millam, J. M.; Iyengar, S. S.; Tomasi, J.; Barone, V.; Mennucci, B.; Cossi, M.; Scalmani, G.; Rega, N.; Petersson, G. A.; Nakatsuji, H.; Hada, M.; Ehara, M.; Toyota, K.; Fukuda, R.; Hasegawa, J.; Ishida, M.; Nakajima, T.; Honda, Y.; Kitao, O.; Nakai, H.; Klene, M.; Li, X.; Knox, J. E.; Hratchian, H. P.; Cross, J. B.; Adamo, C.; Jaramillo, J.; Gomperts, R.; Stratmann, R. E.; Yazyev, O.; Austin, A. J.; Cammi, R.; Pomelli, C.; Ochterski, J. W.; Ayala, P. Y.; Morokuma, K.; Voth, G. A.; Salvador, P.; Dannenberg, J. J.; Zakrzewski, V. G.; Dapprich, S.; Daniels, A. D.; Strain, M. C.; Farkas, O.; Malick, D. K.; Rabuck, A. D.; Raghavachari, K.; Foresman, J. B.; Ortiz, J. V.; Cui, Q.; Baboul, A. G.; Clifford, S.; Cioslowski, J.; Stefanov, B. B.; Liu, G.; Liashenko, A.; Piskorz, P.; Komaromi, I.; Martin, R. L.; Fox, D. J.; Keith, T.; Al-Laham, M. A.; Peng, C. Y.; Nanayakkara, A.; Challacombe, M.; Gill, P. M. W.; Johnson, B.; Chen, W.; Wong, M. W.; Gonzalez, C.; Pople, J. A. *Gaussian 03, Revision C. 01*; Gaussian Inc.: Pittsburgh, PA, 2003.
35. (1) Becke, A. D. Density-Functional Thermochemistry. III. The Role of Exact Exchange. *J. Chem. Phys.* **1993,** *98*, 5648–5652; (b) Lee, C.; Yang, W.; Parr, R. G. Development of the Colle-Salvetti Correlation-Energy Formula into a Functional of the Electron Density. *Phys. Rev. B* **1988,** *37*, 785–789; (c) Vosko, S. H.; Wilk, L.; Nusair, M. Accurate Spin-Dependent Electron Liquid Correlation Energies for Local Spin Density Calculations: A Critical Analysis. *Can. J. Phys.* **1980,** *58*, 1200–1211; (d) Stephens, P. J.; Devlin, F. J.; Chabalowski, C. F.; Frisch, M. J. Ab Initio Calculation of Vibrational Absorption and Circular Dichroism Spectra Using Density Functional Force-Fields. *J. Phys. Chem.* **1994,** *98*, 11623–11627.
36. (a) Dunning, T. H. Jr. Gaussian Basis Functions for Use in Molecular Calculations. I. Contraction of (9s5p) Atomic Basis Sets for the First-Row Atoms. *J. Chem. Phys.* **1970,** *53*, 2823–2833; (b) Dunning, T. H. Jr.; Hay, P. J. Gaussian Basis Set for Molecular Calculations. In: *Modern Theoretical Chemistry*, Vol. III, Chap. 1: Methods of Electronic Structure Theory, Schaefer, H.F. III, Ed.; Plenum Press: New York, 1977.
37. Clark, T.; Chandrasekhar, J.; Spitznagel, G. W.; von Schleyer, P. R. Efficient Diffuse Function-Augmented Basis Set for Anion Calculations. III. The 3-21 + G Basis Set for the First-Row Elements, Lithium to Fluorine. *J. Comp. Chem.* **1983,** *4*, 294–301.
38. (a) Bergner, A.; Dolg, M.; Kuechle, W.; Stoll, H.; Preuss, H. Ab Initio Energy-Adjusted Pseudopotentials for Elements of Groups 13–17. *Mol. Phys.* **1983,** *80*, 1431–1441; (b) Dolg, M.; Stoll, H.; Preuss, H.; Pitzer, R. M. Relativistic and Correlation Effects for Element 105 (hahnium, Ha): A Comparative Study of M and MO (M = Nb, Ta, Ha) Using Energy-Adjusted Ab Initio Pseudopotentials. *J. Phys. Chem.* **1993,** *97*, 5852–5859.
39. Glendening, E. D.; Feller, D.; Thompson, M. A. An Ab Initio Investigation of the Structure and Alkali Metal Cation Selectivity of 18-Crown-6. *J. Am. Chem. Soc.* **1994,** *116*, 10657–10659.
40. (a) Weigend, F.; Ahlrichs, R. Balanced Basis Sets of Split Valence, Triple Zeta Valence and Quadruple Zeta Valence. *Phys. Chem. Chem. Phys.* **2005,** *7*, 3297–3305; (b) Schaefer, A.; Huber, C.; Ahlrichs, R. Fully Optimized Contracted Gaussian Basis Set of Triple Zeta Valence. *J. Chem. Phys.* **1994,** *100*, 5829–5835.
41. (a) Feller, D. The Role of Databases in Support of Computational Chemistry Calculations. *J. Comp. Chem.* **1996,** *17*, 1571–1586; (b) Schuchardt, K. L.; Didier, B. T.; Elsethagen, T.; Sun, L.; Gurumoorthi, V.; Chase, J.; Li, J.; Windus, T. L. Basis Set Exchange: A Community Database for Computational Sciences. *J. Chem. Inf. Model* **2007,** *47*, 1045–1052.
42. Leininger, T.; Nicklass, A.; Kuechle, W.; Stoll, H.; Dolg, M.; Bergner, A. The Accuracy of the Pseudopotential Approximation: Non-Frozen-Core Effects for Spectroscopic Constant of Alkali Fluorides XF (X = K, Rb, Cs). *Chem. Phys. Lett.* **1996,** *255*, 274–280.
43. Peterson, K. A.; Figgen, D.; Goll, E.; Stoll, H.; Dolg, M. Systematically Convergent Basis Set with Relativistic Pseudopotentials. II Small-Core Pseudopotentials and Correlation Consistent Basis Set for the Post-d Group 16–18 Elements. *J. Chem. Phys.* **2003,** *119*, 11113–11123.
44. (a) Armentrout, P. B. Is the Kinetic Method a Thermodynamic Method? *J. Mass Spectrom.* **1999,** *34*, 74–78; (b) Drahos, L.; Vékey, K. How Closely Related are the Effective and the Real Temperature. *J. Mass Spectrom.*

1999, *34*, 79–84; (c) Cooks, R. G.; Koskinen, J. T.; Thomas, P. D. The Kinetic Method of Making Thermochemical Determinations. *J. Mass Spectrom.* **1999,** *34*, 85–92.
45. Ma, J. C.; Dougherty, D. A. The Cation/π Interaction. *Chem. Rev.* **1997,** *97*, 1303–1324.
46. Gal, J. F.; Maria, P. C.; Decouzon, M.; Mo, O.; Yanez, M. Gas-Phase Lithium-Cation Basicities of Some Benzene Derivatives. An Experimental and Theoretical Study. *Int. J. Mass Spectrom. Ion Processes* **2002,** *219*, 445–456.
47. (a) Amunugama, R.; Rodgers, M. T. Influence of Substituents on Cation/π Interactions. I. Absolute Binding Energies of Alkali Metal Cation-Toluene Complexes Determined by Threshold Collision-Induced Dissociation and Theoretical Studies. *J. Phys. Chem. A* **2002,** *106*, 5529–5539; (b) Amunugama, R.; Rodgers, M. T. Influence of Substituents on Cation/π Interactions. II. Absolute Binding Energies of Alkali Metal Cation-Fluorobenzene Complexes Determined by Threshold Collision-Induced Dissociation and Theoretical Studies. *J. Phys. Chem. A* **2002,** *106*, 9092–9103; (c) Amunugama, R.; Rodgers, M. T. The Influence of Substituents on Cation/π Interactions. IV. Absolute Binding Energies of Alkali Metal Cation-Phenol Complexes Determined by Threshold Collision-Induced Dissociation and Theoretical Studies. *J. Phys. Chem. A* **2002,** *106*, 9718–9728; (d) Amunugama, R.; Rodgers, M. T. Influence of Substituents on Cation/π Interactions. III. Absolute Binding Energies of Alkali Metal Cation-Aniline Complexes Determined by Threshold Collision-Induced Dissociation and Theoretical Studies. *Int. J. Mass Spectrom. Ion Processes* **2003,** *227*, 339–360; (e) Amunugama, R.; Rodgers, M. T. Influence of Substituents on Cation/π Interactions. V. Absolute Binding Energies of Alkali Metal Cation-Anisole Complexes Determined by Threshold Collision-Induced Dissociation and Theoretical Studies. *Int. J. Mass Spectrom. Ion Processes* **2003,** *222*, 431–450.
48. McMahon, T. B.; Kebarle, P. Intrinsic Acidities of Substituted Phenols and Benzoic Acids Determined by Gas-Phase Proton-Transfer Equilibria. *J. Am. Chem. Soc.* **1977,** *99*, 2222–2230.
49. Leo, H. A.; Taft, R. W. A Survey of Hammett Substituent Constants and Resonance and Field Parameters. *Chem. Rev.* **1991,** *91*, 165–195.
50. (a) Drahos, L; Vekey, K. Entropy Evaluation Using the Kinetic Method: Is it Feasible? *J. Mass Spectrom.* **2003,** *38*, 1025–1042; (b) Kish, M. M.; Wesdemiotis, C.; Ohanessian, G. The Sodium Ion Affinity of Glycylglycine. *J. Phys. Chem. B* **2004,** *108*, 3086–3091; (c) Bouchoux, G. Evaluation of the Protonation Thermochemistry Obtained by the Extended Kinetic Method. *J. Mass Spectrom.* **2006,** *41*, 1006–1013.